Emergent and animated COLLADA models of the Tonga Trench and Samoa Archipelago: Implications for geoscience modeling, education, and research

Declan G. De Paor*, Steve C. Wild, and Mladen M. Dordevic
Department of Physics, Old Dominion University, Norfolk, Virginia 23529, USA

ABSTRACT

We report on a project aimed at developing emergent animated COLLADA (collaborative design activity) models of the Tonga-Samoa region of the western Pacific for teaching and outreach use with Google Earth. This is an area of historical importance to the development of plate tectonic theory and is important today owing to neotectonic activity, including a 29 September 2009 tsunamigenic earthquake. We created three types of models: an emergent digital elevation model of the Tonga slab with associated magmatic arc and backarc basin based on GeoMapApp (Marine Geoscience Data System, Lamont-Doherty Earth Observatory) data mining; animated models of alternative plate tectonic scenarios; and a large-scale model that permits users to view the subsurface down to lower mantle levels. Our models have been deployed in non–science major laboratory classes, and positive learning outcomes were documented in an independent study by S. Wild and J. Gobert. The models have also been made available to colleagues and the public via the Old Dominion University Pretlow Planetarium and an outreach and dissemination website (http://www.digitalplanet.org). In the process of constructing a complete set of tectonic models for the area of interest, we added cases that have not been described in the research literature. Thus, this study spans the three functions of modern academia, i.e., research, teaching, and outreach, and the multifaceted aspects of creating, using, testing, and disseminating electronic geospatial learning resources.

INTRODUCTION

On 29 September 2009, a deadly tsunamigenic earthquake occurred south of the Pacific islands of Western Samoa and American Samoa, drawing the attention of the world to a region of complex oceanic plate tectonics (Lay et al., 2010; Okal et al., 2010). The magnitude 8.1 earthquake (http://earthquake.usgs.gov/earthquakes/recenteqsww/Quakes/us2009mdbi.php) occurred near the point where the Pacific plate's active western margin turns sharply from a northward-trending convergent boundary to a westward-trending transverse boundary (Fig. 1). Historically, tsunamis in this region are associated only with convergent tectonics. The extensional event (http://earthquake.usgs.gov/earthquakes/recenteqsww/Quakes/us2009mdbi.php#scitech) on 29 September was in a part of the plate subject to significant lithospheric flexure and tangential longitudinal strain, close to but not on the active plate boundary.

Because of the nature of the tectonic setting, we created a set of emergent and animated COLLADA (collaborative design activity) models (Arnaud and Barnes, 2006; De Paor, 2007a, 2007b, 2008a; De Paor et al., 2009a; De Paor and Whitmeyer, 2011a) in Google Earth (http://www.google.com/earth/index.html) that would clearly illustrate the three-dimensional structure and its temporal evolution. Our purpose was principally instruction and outreach, since visualizations have been demonstrated (e.g., Gobert, 2000, 2005) to play a key role in many novices' conceptualization of tectonic movements (however, in the process of designing instructional visualizations, we found that attempting to cover all multiple working hypotheses led us to additional models not previously described in the tectonic literature of the region). Our target audience was threefold: (1) the large number of non-major students who study courses involving plate tectonics as part of their general education requirements in the U.S. undergraduate education system; (2) visitors to the Pretlow Planetarium who can view our models beside models of lunar and planetary structures in a museum-style informal education setting; and (3) visitors to our website (http://www.digitalplanet.org), which is sponsored by the National Science Foundation (NSF) for the purpose of disseminating the results of our funded research. Learning outcomes were tested with the first target audience only and will be reported in an independent study (Gobert et al., 2012; see the following summary). Given the positive learning gains recorded, the visualizations could prove beneficial to other groups, including geoscience majors taking courses in structural geology and tectonics, geophysics, or geodynamics, and citizens ranging from first responders in earthquake- and tsunami-prone regions to casual museum visitors.

We chose to create COLLADA models because they can be viewed with the highly popular Google Earth virtual globe (De Paor, 2007a), the basic version of which is free (the commercial Google Earth Pro can be used to view our models, but it is not required). Google Earth is both a desktop application and a web browser plug-in that contains many built-in geoscience data sets in its primary database, including surface imagery, water bodies, volcanoes, and earthquakes, all of which can be used to study subduction zones and marginal basins. In general, Google Earth is most suited for studying processes at or above the surface (e.g., De Paor et al., 2007; McDonald and De Paor, 2008); however, we have developed several techniques for visualizing the subsurface, as outlined in detail herein (see also De Paor and Pinan-Llamas, 2006; De Paor and Williams, 2006; Whitmeyer and De Paor, 2008; De Paor and Whitmeyer, 2011a).

This paper is aimed toward readers with an interest in the tectonics of the region, those who would like to use the models we have created in their classrooms or informal education settings, and those who want to discover how to create their own three-dimensional (3D) COLLADA models of global-scale processes elsewhere for viewing on Google Earth. In the past, modeling was done mainly by computer programmers; however, just as nontechnical people are increasingly contributing to website content (especially via social media such as Facebook that facilitate easy uploading of custom content), the old dis-

*Corresponding author: ddepaor@odu.edu.

Geosphere; April 2012; v. 8; no. 2; p. 491–506; doi:10.1130/GES00758.1; 23 figures; 5 tables; 10 supplemental files.

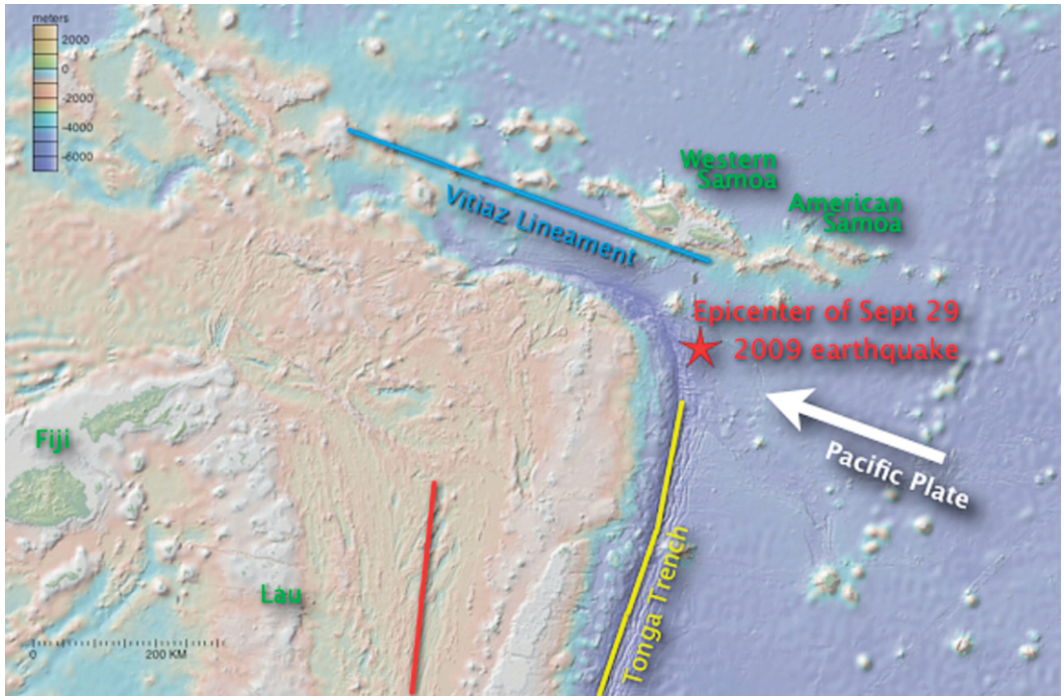

Figure 1. View of Tonga-Samoa region from our data-mining source, GeoMapApp (see text; http://www.geomapapp.org.). Red star marks epicenter of 29 September 2009 tsunamigenic earthquake south of Samoa. Yellow line marks Tonga Trench; red line is center of Lau marginal basin; blue line is Vitiaz Lineament. Principle emergent island names are in green.

tinctions between teacher, researcher, and programmer are breaking down as increasing numbers of academics create, test, and disseminate their own computer-based learning, research, and outreach resources.

GEOLOGICAL BACKGROUND

The Pacific plate (Fig. 2) is formed by the tectonic processes of mantle upwelling, partial melting, crustal magmatism, and seafloor spreading on the western side of the Pacific Ocean Basin spreading ridge, the East Pacific Rise. Unlike the Mid-Atlantic Ridge, which is symmetrically positioned roughly equidistant from the Atlantic Ocean Basin eastern and western passive margins, the East Pacific Rise is located much closer to (in places actually on) the Pacific eastern active margin along the Americas. The Pacific plate thus extends westward across thousands of kilometers of Earth's surface before encountering the various plates and microplates that mark the western active margin of the Pacific Ocean Basin. As it moves away from the spreading ridge, the plate becomes older, colder, thicker, and denser (Parker and Oldenburg, 1973; Yoshii, 1975), and eventually is subducted along the western part of the so-called Pacific Ring of Fire. Owing to variations in strike of the western active margin, tectonism varies in style from convergent to transverse, and associated marginal basins commonly undergo minor divergent tectonism.

In this paper, we focus on a study area (Fig. 3) from longitude 170°W to the antimeridian (180°), and latitude 13°S to the Tropic of Capricorn (23.5°S). The overall structure of the region consists of (1) the westward spreading Pacific plate, (2) the older extension of that plate north of American Samoa, (3) the Tonga-Kermadec trench, (4) the Tonga volcanic arc, (5) the Lau backarc basin, (6) the Lau remnant arc, and (7) the South Fiji Basin.

A complication occurs south of this study region, where a line of seamounts is currently subducting near Monowai, resulting in the differentiation of the northern Tonga and southern Kermadec Trenches. To avoid this complexity, our study is confined to the region north of Monowai. To the west, the Lau backarc basin meets the South Fiji Basin, which is influenced by subduction of opposite polarity from the New Hebrides convergent zone farther west. Our study area is thus strategically chosen to avoid unnecessary complications.

In all but the northernmost part of our study area, the ~100-m.y.-old Cretaceous crust of the Pacific plate meets the recently formed edge of the Indo-Australian plate along a 6–10 km

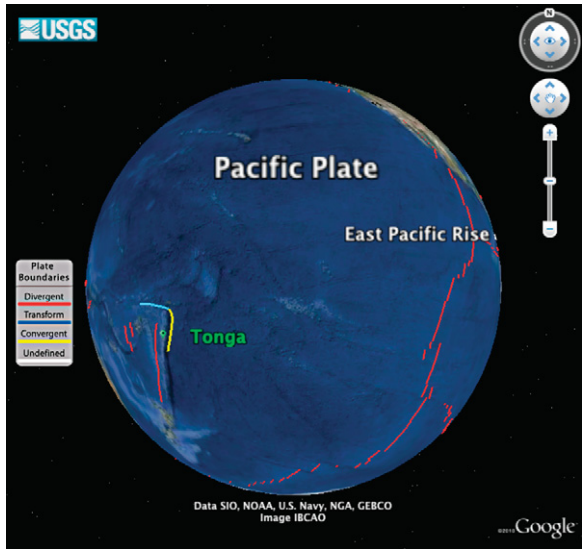

Figure 2. Google Earth representation of tectonics of Pacific Ocean Basin. Red lines mark East Pacific Rise. Northern Tonga Trench shown in yellow, Samoan transform boundary in cyan. Island of Tonga indicated in green. Modified from KML (Keyhole Markup Language) file downloaded from U.S. Geological Survey at http://earthquake.usgs.gov/regional/nca/virtualtour/kml/plateboundaries.kmz.

bathymetric depression called the Tonga Trench (Muller et al., 2008). A 100-km-thick descending lithospheric slab dips westward under the Lau Basin to form the Tonga subduction zone. Slab morphology has been determined to various mantle depths (Gudmundsson and Sambridge, 1998; Syracuse and Abers, 2006) and data are readily available in the GeoMapApp (Marine Geoscience Data System, Lamont-Doherty Earth Observatory) online database (http://www.geomapapp.org; Ryan et al., 2009).

The chosen study area is of interest for several reasons. It is important for the scientific history of the theory of plate tectonics because seismic studies in this region were the basis for the original identification of subduction by Isacks et al. (1968). The relationships illustrated within the dotted parallelogram of Figure 4 (modified slightly from the illustration in Isacks et al., 1968) were inspired by the Tonga-Samoa region. Furthermore, the Lau Basin is a classic teaching example of backarc spreading due to trench rollback and trench suction (Uyeda and Kanamori, 1979; Rosenbaum and Lister, 2004; Moores and Twiss, 1995). In the rollback process, the immaterial line of maximum lithospheric flexure entering the trench migrates horizontally eastward as material in the plate continues to travel westward and turn downward. This creates a so-called trench suction force that extends the overlying arc and causes divergence in the backarc basin (Fig. 5). Rollback is a spatiotemporal concept involving different directions and rates of movement of material versus immaterial geometries, and is thus potentially difficult to visualize, even by experts.

Toward the north, the Tonga Trench ends abruptly along the Vitiaz Lineament just south of the approximately east-west–trending Samoa Archipelago of islands and seamounts (Figs. 1 and 3). Here, the strike of the convergent plate boundary turns sharply from north to west, to become parallel to the plate movement vector, and the boundary transitions into a transform boundary. North of this latitude and continuing beyond the study area, the Pacific plate forms the ocean floor for thousands of kilometers westward, progressively aging from Cretaceous to Jurassic before subducting at locations such as the Mariana Trench, whereas to the south of the Vitiaz Lineament, the 6-m.y.-old Cenozoic marginal Lau Basin overlies the subducting Tonga slab (Lupton et al., 2004; German et al., 2006), dividing the active Tonga volcanic arc to its east from the extinct Lau arc to its west.

The change from convergent to transform plate margin correlates with geophysical evidence (Smith et al., 2001) that the lithosphere is in the process of tearing just southwest of

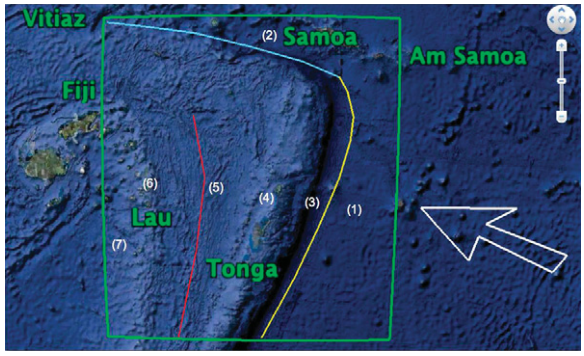

Figure 3. Current study area outlined in green. Pacific plate motion direction in white. Yellow line marks Tonga Trench, cyan line is Vitiaz Lineament. Red line represents complex region of backarc spreading. Am—American. Numbers 1–7 correlate with regions described in Geological Background discussion.

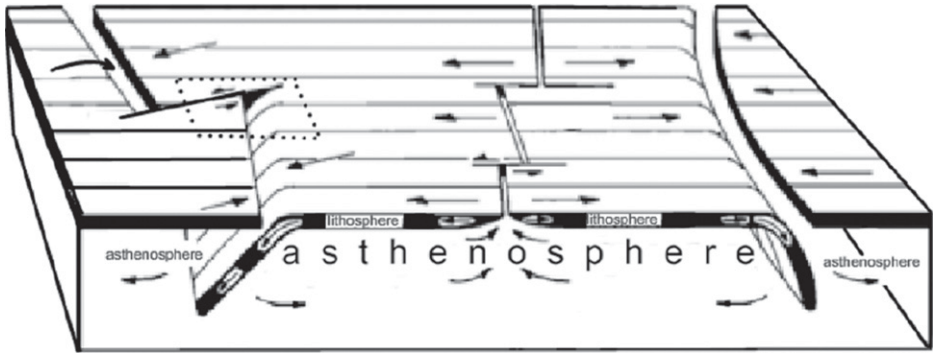

Figure 4. Plate tectonics explained in famous illustration (slightly modified) from Isacks et al. (1968, their fig. 1). Width of Pacific plate is not to scale. Asymmetric position of East Pacific Rise is not shown. Dotted parallelogram marks present study area.

American Samoa (Fig. 6). An instructional analogy can be created easily, either by cutting partially through a sheet of paper or wood panel, or by holding one's fingers as shown in Figure 6 (inset). However, the transition is complicated and obscured because the Vitiaz Lineament has been alternately interpreted as a dormant compressional structure dating from times when plate movement vectors were different (Pelletier and Auzende, 1996), or a product of rapid eastward tearing of the lithosphere (Hart et al., 2004).

At the northern end of the Tonga Trench, rates of subduction exceeding 200 mm/yr are among the highest documented anywhere on Earth (van der Hilst, 1995; Muller et al., 2008; Bonnardot et al., 2009). Holt (1995) noted a south to north increase in downdip velocities of the slab, and the widening of the Lau backarc basin is consistent with a northward increase

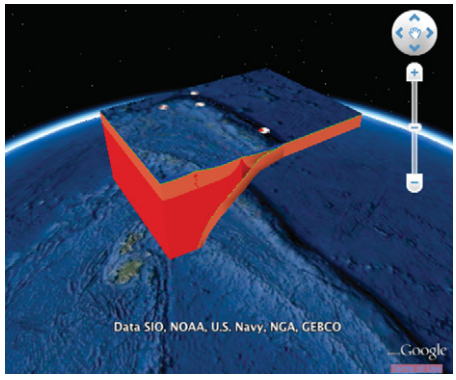

Figure 5. COLLADA (collaborative design activity) models raised above Google Earth surface showing structure of study region. Arc, basin, and slab can be selectively shown or hidden.

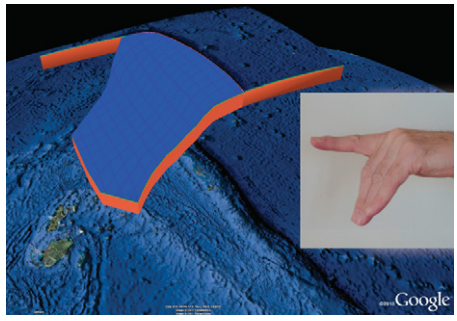

Figure 6. Hiding Tonga arc and Lau Basin reveals how southern (nearer) portion of Pacific plate subducts along Tonga Trench while northern part continues westward on Earth's surface. Inset: hand analogy helps some students visualize situation.

in the rate of rollback, as high as 100 mm/yr. The trench continues along strike to the south beyond the study area, where it is known as the Kermadec Trench. However, the character of the downgoing slab varies along strike, as revealed by seismic tomography (Fig. 7). Tomography shows a lithospheric slab dipping steeply all the way down to mid-mantle levels (1600 km out of the mantle total of 2981 km) south of Tonga, whereas in the current study area a shallow segment is imaged in the 410–660 km transition zone (van der Hilst, 1995; Mussett and Khan, 2000). These depths correspond to the olivine-spinel and spinel-perovskite phase transitions, which are thought to affect slab density and kinematics. Bonnardot et al. (2009) presented evidence of slab detachment at intermediate depths.

The Samoa Archipelago of islands and seamounts that forms the northernmost strip of the study area has been interpreted alternatively as attributable to drift of the Pacific plate over a deep-seated Samoan hotspot analogous to the Hawaiian hotspot (McDougall, 2010) or as a result of warping and stretching along an east-west–trending lithospheric monocline in the proximity of the transform boundary and tear point (Hart et al., 2004). In either case, the volcanic lineament adds complexity and intrigue to the story of this region.

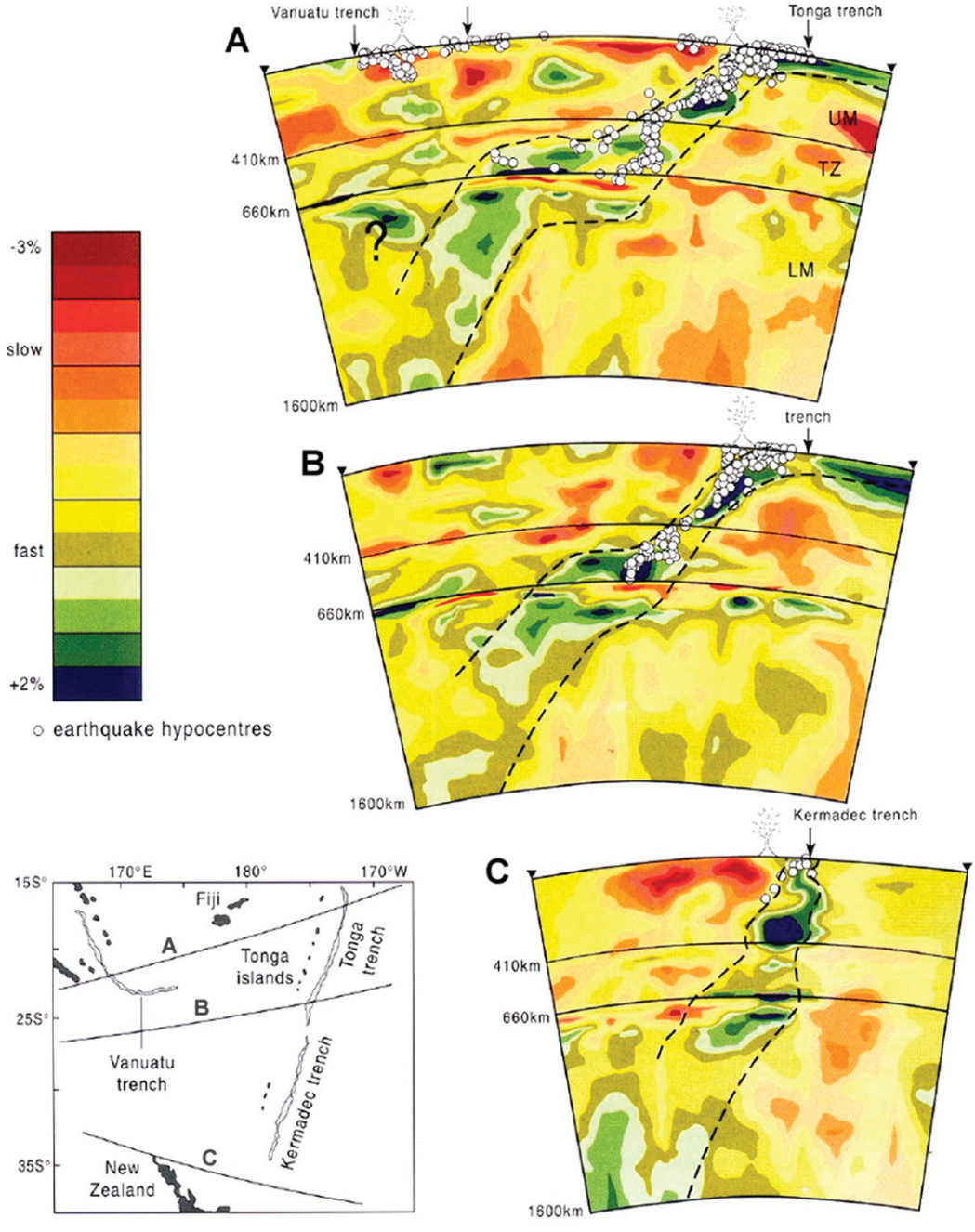

Figure 7. Seismic tomography of Tonga-Kermadec slab, reproduced from Mussett and Khan (2000). Note mid-mantle flat slab developed in north but not in south.

COLLADA MODELS IN THE GOOGLE EARTH DESKTOP APPLICATION

To aid with visualization of complex tectonics, we constructed interactive emergent and animated COLLADA models of the Tonga-Samoa region. We include a description of the model coding process here both for those readers who are interested in how COLLADA works and for those who might wish to create similar models elsewhere. Our experiences in copresenting several oversubscribed Geological Society of America short courses and workshops on the topic of Google Earth modeling with COLLADA point to the growing interest in this approach among geoscience researchers and educators. The following account should be accessible to readers without experience in programming languages such as FORTRAN or C. If readers can format a website page with HTML (Hypertext Markup Language), they can modify the types of scripts discussed herein to work in their own area of interest (for more details of scripting for Google Earth, see Wernecke, 2009; De Paor and Whitmeyer, 2011a).

One of the more powerful features of Google Earth is the ability it offers users to display their own content (Goodchild, 2008). Custom content can be added using Google Earth's menus or by creating a file written in the Keyhole Markup Language (KML), a dialect of XML (Extensible Markup Language) designed specifically for virtual globes. The basic structure of a KML file is shown in Table 1. This script places a default yellow map pin in the center of North America. The custom content we are most interested in here consists of 3D COLLADA models. Like KML, COLLADA is another dialect of XML and is used mainly to add 3D buildings to Google Earth, for example using the Google SketchUp modeling program (http://sketchup.google.com). Fortunately, the dimensions of COLLADA models can be regional or global in magnitude, so that a program intended for modeling buildings can be used to create crustal blocks on the scale of mountains (De Paor, 2008b, and "Using Google SketchUp with Google Earth for scientific applications" discussed in Google Tech Talk: http://www.youtube.com/watch?v=6cVJqvsfxvo) or even continents (Dordevic et al., 2009, 2010; De Paor et al., 2011). COLLADA models saved in Digital Asset Exchange (DAE) files are recognized and imported by Google Earth. The example in Table 2 adds a model of the Tonga slab as seen in Figure 6.

TABLE 1. PLACEMARK

```
<?xml version="1.0"?>
<kml>
        <Document>
                <Placemark>
                        <Point>
                                <coordinates>-95.45, 37.68, 0</coordinates>
                        </Point>
                </Placemark>
        </Document>
</kml>
```

TABLE 2. COLLADA MODEL

```
<?xml version="1.0"?>
<kml>
        <Placemark>
                <Model>
                        <altitudeMode>relativeToSeaFloor</altitudeMode>
                        <Location>
                                <longitude>85.935848221848</longitude>
                                <latitude>-18.36255792927627</latitude>
                                <altitude>200000</altitude>
                        </Location>
                        <Orientation>
                                <heading>21.732</heading>
                                <tilt>0</tilt>
                                <roll>0</roll>
                        </Orientation>
                        <Scale>
                                <x>0.816</x>
                                <y>0.776</y>
                                <z>0.796</z>
                        </Scale>
                        <Link>
                                <href>files/TongaSlab.dae</href>
                        </Link>
                </Model>
        </Placemark>
</kml>
```

To create Figure 6, we digitally mined data from Syracuse and Abers (2006) that are openly available on GeoMapApp (http://www.geomapapp.org). GeoMapApp is a free desktop application that gives the user a Google Maps–style interface with a wide range of geological data (Fig. 1 is a screen shot). Among the global data sets made accessible in GeoMapApp are earthquake hypocenters. The first step to creating our models was to select a rectangular region in GeoMapApp, export the hypocenter points, and load them into an Excel file. This file was used to create points with correct depth tags for compatibility with KML. Once the points were in the KML file, a snapshot of the region of interest was taken in Google Earth. This picture was saved as a PNG (Portable Network Graphics) image file, which was then edited with photographic editing software. We used the free open-source application called GIMP (GNU Image Manipulation Program; http://www.gimp.org); however, owners of a commercial application such as Adobe Photoshop could use it equally well. In Google SketchUp, a rectangle was created with the same dimensions as the area from which the Google Earth terrain image was taken. The edited PNG file was then used as a so-called texture pasted on the rectangle (i.e., an image covering a model surface like wallpaper). In the case of the GeoMapApp data, to aid computer memory management several small sections were exported onto six different rectangles. Next, points were dropped to the correct depth beneath the surface. If several data were clustered together the deepest one was selected (usually the depths were within 5 km of one another). After all the points were correctly located in the z-dimension, the regions were stitched together using geological markers and longitude and latitude lines. The data points were then connected into depth profile lines. An outline of the surface slab was copied and offset 5 km to simulate ocean crustal thickness and a second copy of the slab was offset 100 km to create a bounding surface at the bottom of the lithosphere. These slab surfaces were intersected by vertical planes on the sides using a Google SketchUp "intersect" command to complete a solid model. The georeferenced slab was saved in a DAE file, which was imported into Google Earth.

A similar process was used to create 3D models of the arcs and backarc basin, except that these were constrained by the subducting slab geometry, not by seismic data. Finally, a KML "Placemark" element containing the model (Table 2) was replicated and a KML "TimeSpan" element was added to each replica Placemark (Table 3). The begin and end time tags of the TimeSpan and the model's altitude

tag were incremented in unison (in KML, the altitude is in meters, so 200000 represents an altitude of 200 km). As the Google Earth slider is moved and a slider value is reached, the code responds by changing the elevation of the COLLADA model. All tectonic domains were elevated in unison, but different domains were placed in separate KML folders so that they could be selectively shown or hidden.

Two difficulties were encountered in this process. First, the study area bordered the Earth's antimeridian and Google Earth was found to behave erratically in this region. We overcame this by draping the famous National Aeronautics and Space Administration (NASA) "Blue Marble" image of the Earth (http://www.nasa.gov/images/content/136215main_BMarbleStill.jpg) over the Google Earth surface imagery and moving the origin of longitude so that the models were safely away from the antimeridian (a second ground overlay snapped from the Google Earth terrain was superimposed in the Tonga region in order to provide local detail; Fig. 8). A side effect of this solution is that the latitude-longitude grid must be left turned off. The second difficulty was that the time slider technique gave the viewer only one slider control, whereas we wanted to be able to both elevate and animate the block. Initially, we animated blocks that were already elevated to a fixed altitude (Supplemental Movie 1) but later we switched to the Google Earth application programming interface (API; see next section).

Animating models in Google Earth (Table 4) was similar to elevating emergent models (Table 3). Instead of incrementing the altitude of a single model, we created a sequence of gradually differing models at a constant altitude (a marker was used to ensure that models were all exported from the same spot to prevent unwanted jittering or wobble), and we changed the name of the linked model file in the KML Placemark sequence. This introduced an unanticipated problem. Although the images used as textures were relatively small (under 100 kilobytes), the long sequence of models used in this animation proved to be hesitant to load even on a fast computer. Google Earth displayed the blank, white-sided model frame first and applied texture images after a brief interval. Even though this was <1 s in most cases, white flashes interrupted the immersive effect of the animation. Our solution was to wait for all frames to load before playing the animation; however, this approach is tedious. Hopefully, future versions of Google Earth will cache textures before displaying models or build visualizations in an off-screen bitmap and only move them on screen completely loaded; this is standard practice in other applications.

TABLE 3. EMERGENT COLLADA MODEL

```
<?xml version="1.0"?>
<kml>
        <Placemark>
                <TimeSpan>
                        <begin>-100</begin>
                        <end>-200</end>
                </TimeSpan>
                <Model>
                        ...
                        <Location>
                                <longitude>...</longitude>
                                <latitude>...</latitude>
                                <altitude>200000</altitude>
                                ...
                                ...
                                ...
        </Placemark>
        <Placemark>
                <TimeSpan>
                        <begin>-200</begin>
                        <end>-300</end>
                </TimeSpan>
                <Model>
                        ...
                        <Location>
                                <longitude>...</longitude>
                                <latitude>...</latitude>
                                <altitude>300000</altitude>
                                ...
                                ...
                                ...
```

GOOGLE EARTH API AND JAVASCRIPT CONTROLS

In addition to the well-known stand-alone desktop application, Google Earth is available as a web browser plug-in that allows one or more instances of the virtual globe to be embedded in a website page and controlled with client-side JavaScript (a sample script is shown in Table 5) or by means of server-side scripts written with a scripting language such

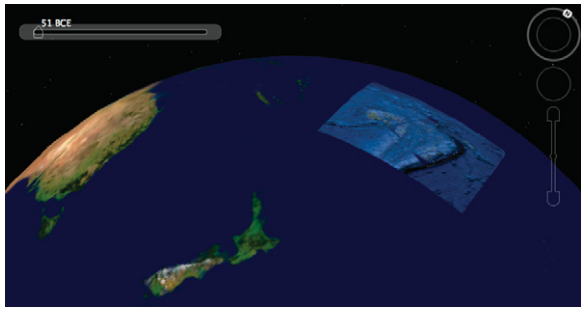

Figure 8. Seafloor detail for Tonga region snapped from Google Earth and draped over National Aeronautics and Space Administration (NASA) "Blue Marble" image of Earth. Both were moved through longitude to get away from the antimeridian, a region where Google Earth has difficulty handling models (see text).

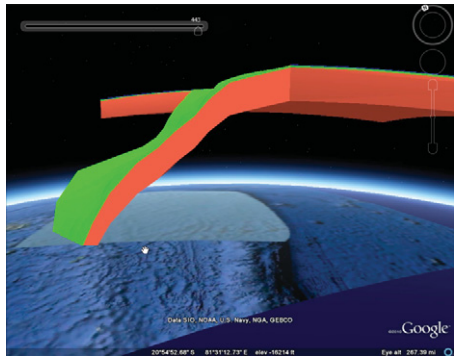

Supplemental Movie 1. MOV video file showing an example of the models used by Gobert et al. (2012) in lab exercises. This movie records a student elevating the Tonga Slab using the Google Earth desktop application. Note the use of the time slider to animate the model. Various pieces can be shown or hidden. To view this file, you will need Quicktime (see www.apple.com/quicktime). If you are viewing the PDF of this paper or reading it offline, please visit http://dx.doi.org/10.1130/GES00758.S1 or the full-text article on www.gsapubs.org to view Supplemental Movie 1.

TABLE 4. ANIMATED COLLADA MODEL

```
<?xml version="1.0"?>
<kml>
        <Placemark>
                <TimeSpan>
                        <begin>-100</begin>
                        <end>-200</end>
                </TimeSpan>
                <Model>
                        ...
                        ...
                        ...
                        <Link>
                                <href>files/200.dae</href>
                                ...
                                ...
                                ...
        </Placemark>
        <Placemark>
                <TimeSpan>
                        <begin>-200</begin>
                        <end>-300</end>
                </TimeSpan>
                <Model>
                        ...
                        ...
                        ...
                        <Link>
                                <href>files/300.dae</href>
                                ...
                                ...
                                ...
```

as PHP (hypertext preprocessor), Python, or Ruby. All features do not transfer over from the Google Earth desktop application to the Google Earth API. There is no sidebar with panels entitled "Search," "Place," and "Layers." However, individual features such as tools in the application toolbar may be coded in JavaScript. Content control using JavaScript is an advantage to the API. Maps, cross sections, and COLLADA models can be independently controlled and modified. Ease of viewing content is a great advantage to the Google Earth API. A person wishing to display content no longer has to download and launch a file, but can view Google Earth directly in their web browser. The Google Earth API is controlled by standard controls found in HTML forms (e.g., buttons, sliders, menus, text boxes). This style of control enables the creation of more robust user interaction with the content. Thus, in the Google Earth API a new control may be added for every user interaction needed. The main controls used in our time-evolved models are the elevation control with a slider and visibility and time and motion controls with buttons. The slider works by allowing the user to vary any KML element over a range of values; for example, it would not be difficult for readers to add their own spot quizzes or text areas for gathering student responses.

For our elevation slider we used an inexpensive commercial product called TigraSlider Control (http://www.softcomplex.com/products/tigra_slider_control). A free version is offered but does not have the necessary functionality. Were we starting fresh, we would use the free native slider input built into HTML5 and supported by all new browsers. Such a slider can be added to a web page with the single line: <input name = "slider" type = "range" min = "0" max = "10" value = "5"> and its value can be read with the JavaScript function document.getElementById('slider').value. The visibility controls are standard HTML form buttons that enable model components to be shown or hidden, thus revealing or obscuring sections of the model behind them. A quick method used to accomplish this task was to change the HTML href hyperlink to the .dae file. If a model component needed to be invisible, the href link was pointed to a nonexistent .dae file, thus nothing was loaded.

TABLE 5. GOOGLE EARTH'S JAVASCRIPT APPLICATION PROGRAM INTERFACE (API)

```
<!DOCTYPE html ...>
<htmL>
        <head>
                <script language="JavaScript" type="text/javascript" src=
"http://www.lions.odu.edu/org/planetarium/steve/Tonga_API/tonga_roll_js/openfile.js">
                </script>
        </head>
        <body>
                <form>
                        <input type="button" value="Load Case 1" onclick="openfile(1)">
                </form>
        </body>
</html>
```

IMPLEMENTATION

Since 2008, we (and our colleagues; Whitmeyer et al., 2011) have been distributing geological COLLADA models to a cohort of educators in a variety of universities and colleges, and we have made them freely available for download both from our academic websites and from www.digitalplanet.org. The animated emergent models described here, along with similar models in a variety of tectonic settings, have been used by us in several undergraduate courses at four east coast universities and are available to visitors to the Old Dominion University Pretlow Planetarium in an informal education setting. During a leave of absence by De Paor in 2010, Wild developed a set of Google Earth API–based laboratory activities including animations using the preceding technique (see Figs. 9, 10, and 11; http://www.lions.odu.edu/org/planetarium/steve/Tonga_API/Tonga_Master.html; Supplemental Movies 1, 2, and 3). These were combined in a single laboratory class along with similar activities addressing the Iceland spreading ridge and hotspot, and presented as a test with IRB (Institutional Review Board) compliance to 127 non–science majors as part of a broad survey of the solar system. Pretests and posttests were administered by Wild and analyzed by NSF-sponsored independent assessor J. Gobert, and they found: 1) overall learning gains; 2) no differences in learning gains when comparing those with prior coursework in geology or geography to students without this prior coursework; and 3) no differences in learning gains when comparing males and females. They report a gender difference favoring males in terms of items completed during the class period and a correlation between students' pretest and embedded laboratory scores (Gobert et al., 2012).

Testing in the informal education setting of a planetarium has not yet been attempted; in a planetarium, models can be displayed on a portion of the dome using a peripheral LCD projector during planetarium shows and on peripheral computer screens that visitors can casually browse. Future plans include eye-tracking studies of such browsing, as we have recently acquired the necessary equipment.

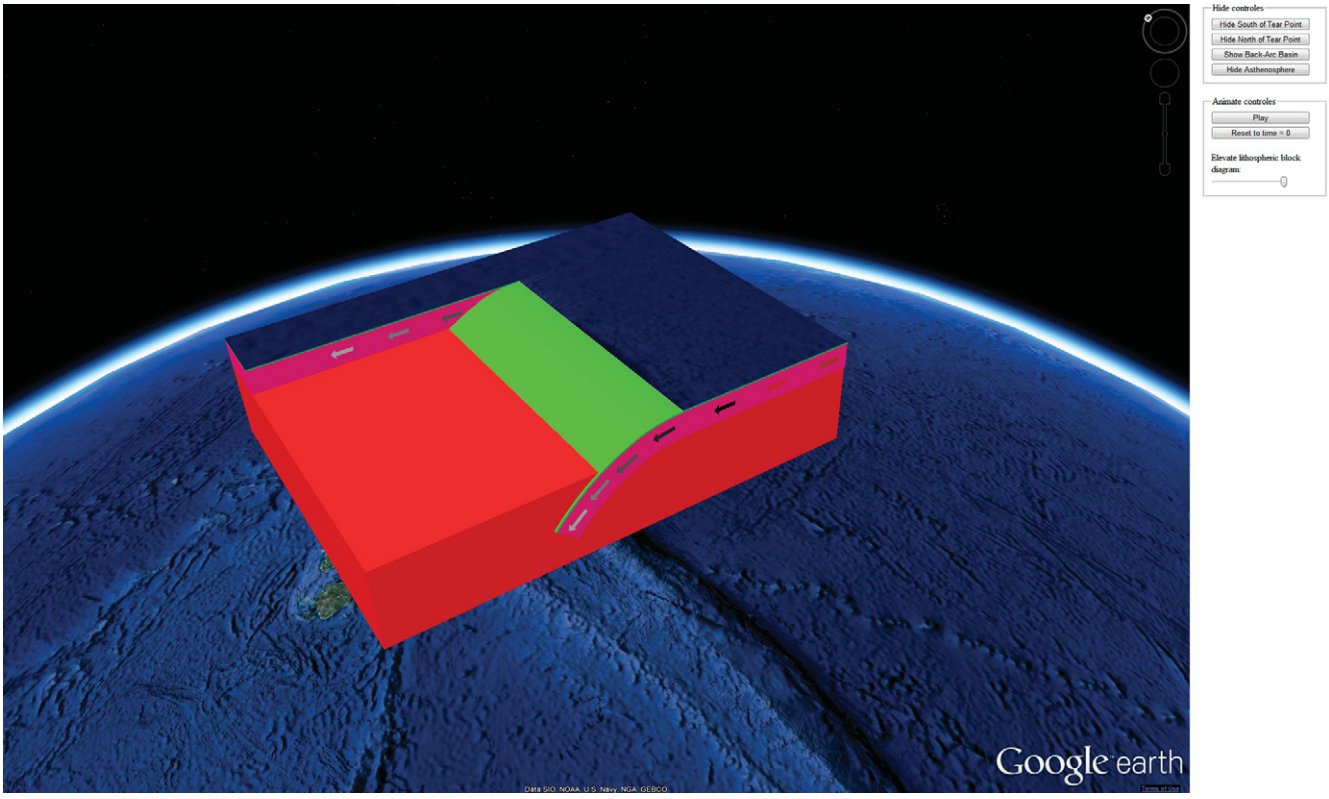

Figure 9. Google Earth API (application programming interface) and COLLADA (collaborative design activity) models manipulated in Google Earth instance embedded in web page. Slider, buttons controlled using JavaScript.

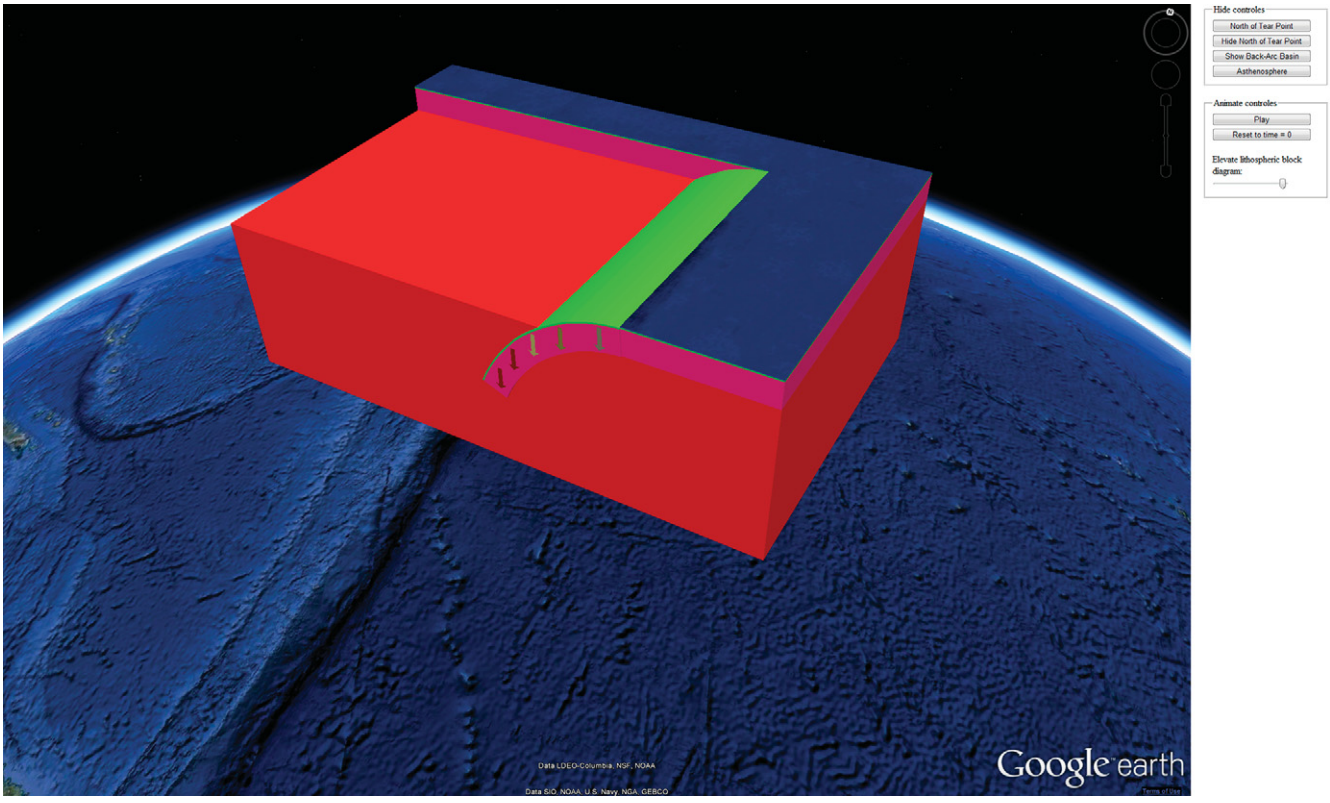

Figure 10. Alternative models of trench rollback and slab kinematics (see text).

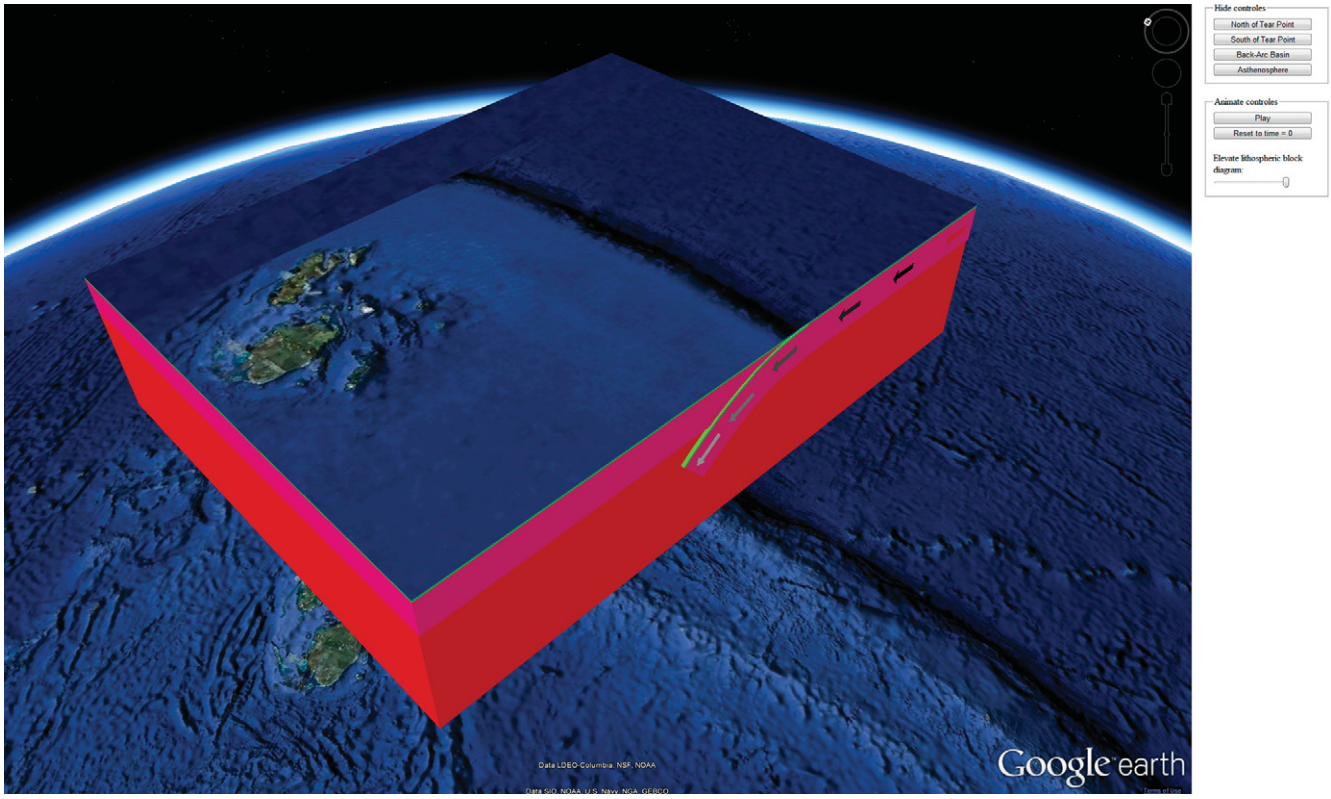

Figure 11. Block model that can be raised and reoriented while animation is running using multiple JavaScript controls.

ENHANCING THE VISUALIZATION USING GOOGLE MARS

In addition to the emergent COLLADA models described here, we developed methods of viewing subsurface tectonic structures in situ. The radius of Earth's outer core (3500 km) is within 3% of the mean radius of Mars. Consequently we can use the Google Mars virtual globe to represent Earth's core-mantle boundary. The martian 3D terrain is turned off and a plain image overlay is used to cover all of the built-in martian surface imagery. At the Earth's core-mantle boundary depth of 2900 km, the peak black-body radiation is white hot; however, white is not a suitable color for modeling, so we use red or gray overlay images (Fig. 12) to convey temperature or metallicity, respectively. An informal poll (taken by De Paor et al., 2011) revealed that 10 of the 14 voters favored the red core, whereas 3 favored gray and 1 favored white). A spherical COLLADA model representing Earth's surface to scale is draped with a semitransparent PNG image of the NASA Blue Marble photo. Figure 13 shows the core with three slices of the mantle under Tonga. The upper part of each slice is textured with seismic tomography from Mussett and Khan (2000). The lower part is colored purple to emphasize the relative proportion of

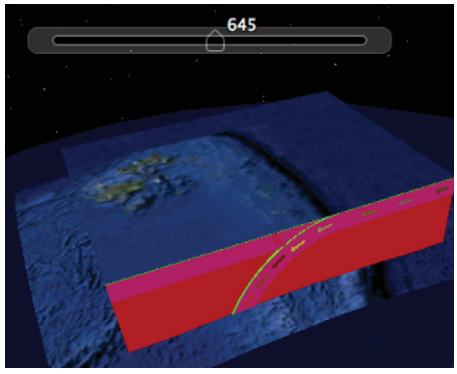

Supplemental Movie 2. MOV video file of a model being animated using the desktop application's time slider. Because there is only one time slider, the model can be elevated or animated, but not both. To view this file, you will need Quicktime (see www.apple.com/quicktime). If you are viewing the PDF of this paper or reading it offline, please visit http://dx.doi.org/10.1130/GES00758.S2 or the full-text article on www.gsapubs.org to view Supplemental Movie 2.

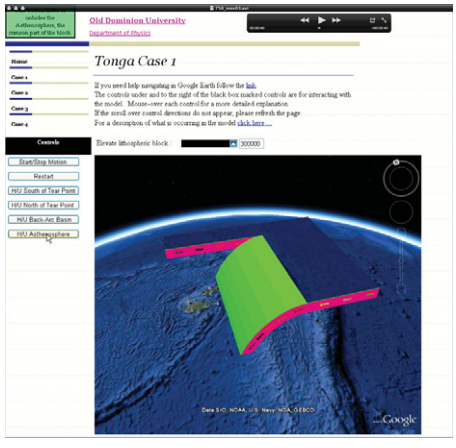

Supplemental Movie 3. MOV file of a model being manipulated using the Google Earth web browser plug-in. The model is both elevated and animated. Various pieces can be shown or hidden. To view this file, you will need Quicktime (see www.apple.com/quicktime). If you are viewing the PDF of this paper or reading it offline, please visit http://dx.doi.org/10.1130/GES00758.S3 or the full-text article on www.gsapubs.org to view Supplemental Movie 3.

the mantle not reached by the tomographic data. Elements of Figures 12 and 13 are combined in Figure 14, with a circular cut-out revealing the interior. All three models can be downloaded from our website (http://www.digitalplanet.org/DigitalPlanet/New-June.html).

The advantage of switching to the martian virtual globe is that the users can fly to placemarks with text balloons, image files, virtual specimens, and COLLADA models representing crustal and mantle features. Although they are actually under the Earth's surface, these placemarks are above the martian virtual globe's zero elevation, thus avoiding the difficulties of subsurface rendering and touring in Google Earth. Note that the scale of the Google Earth ruler tool remains valid.

Specific to this study area, inclusion of deep mantle tomography led us to consider tectonic models of the Tonga subduction system extending beyond the depth of the Syracuse and Abers (2006) data. The feature of particular interest in the tomographic section is the region of shallow or flat slab dip between 430 km and 670 km, as discussed in the following.

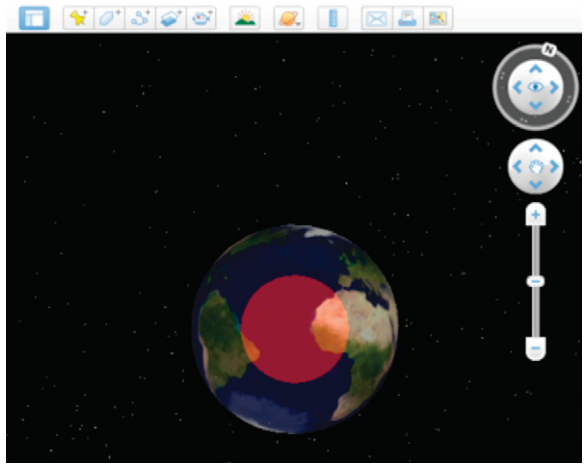

Figure 12. Visualizing subsurface using Google Mars with plain red image overlay and draped over National Aeronautics and Space Administration (NASA) "Blue Marble" image of Earth. COLLADA (collaborative design activity) model of Earth's surface.

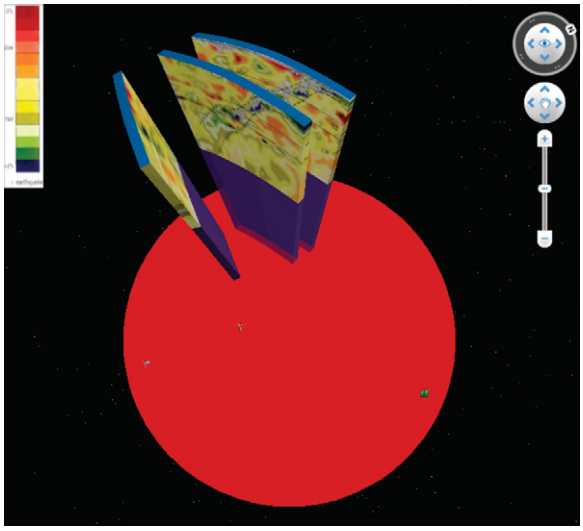

Figure 13. Slices of crust and mantle shown with seismic tomography (from Mussett and Khan, 2000). Note flat subduction at mid-mantle levels. Purple represents lowermost mantle below limit of tomographic data. Red sphere represents Earth's core.

TECTONIC MODELS OF THE TONGA REGION

Creating learning and outreach resources for the Tonga-Samoa region required the assembly of six alternate plate tectonic models, including mostly well-established but also some novel ideas. To a casual observer, this might seem excessive. Geologists are so used to viewing two-dimensional cross sections of subduction zones that they may not ponder how such zones must change in four dimensions of space and time. On a finite spherical Earth, a subduction zone cannot continue along strike forever, and neither Andean-style magmatic arcs (Ramos and Aleman, 2000) nor Lau-style backarc basins (Uyeda and Kanamori, 1979) can be understood in terms of a steady-state subduction system akin to a descending escalator. Yet plate tectonics texts tend to skimp on discussion of complications such as lateral terminations or rollback, and static illustrations strongly suggest a steady-state process of subduction at a fixed trench location. By presenting oversimplified models of subduction to students and the public, we make it impossible for them to truly understand the genesis of arcs.

The rigid Pacific plate is contiguous east of the study area, and its absolute Euler pole of rotation is far away (Fig. 15), so the velocity of the seafloor approaching the Tonga Trench must be approximately the same as its velocity along the Samoa Archipelago north of the subduction zone (http://cais.gsi.go.jp/Virtual_GSI/Tectonics/Pacific_GPS/index.html). Consequently, the variables of interest are the absolute and relative velocities of the tear point. Absolute velocities may be stated relative to the global hotspot reference frame, whereas relative velocities are stated with reference to an arbitrary material point in the lithospheric plate.

Model 1. No Tearing or Slow Tearing

In this end-member case (Fig. 16; Supplemental Model 1[1]), the tear point southwest of American Samoa is not currently active but rides along passively with the plate, a scenario that results in horizontal absolute velocity vectors for all points both on the surface and on the slab. This end-member case cannot be the entire story, because it does not allow subduction to get started in the first place; however, it is a possible temporary condition at some later time. In order for the slab to move horizontally westward, the arc material in front of it must either (1) move west at an equal or greater pace, or else (2) deform to form a contractional forearc accretionary wedge or a foreland thrust belt, or both (Fig. 16). If the tear point propagates eastward more slowly than the plate moves westward, then the movement vectors for material in the slab will dip westward more shallowly than the dip of the slab, and the scenario will also correspond to model 1 (Fig. 17). The structure of the lithosphere above the Tonga subduction

[1]Supplemental Model 1. In this end-member case, the tear point southwest of American Samoa is not currently active but rides along passively with the plate, a scenario that results in horizontal absolute velocity vectors for all points both on the surface and on the slab. See text for details. See also Figure 16. To download the zip file containing the KML file for Supplemental Model 1, please visit http://dx.doi.org/10.1130/GES00758.S4. Or, to view the html file of Supplemental Models 1–6 with a Google Chrome, Firefox, or Safari web browser, please visit http://dx.doi.org/10.1130/GES00758.S5. Both the html file and the zipped file can also be accessed through the full-text article on www.gsapubs.org.

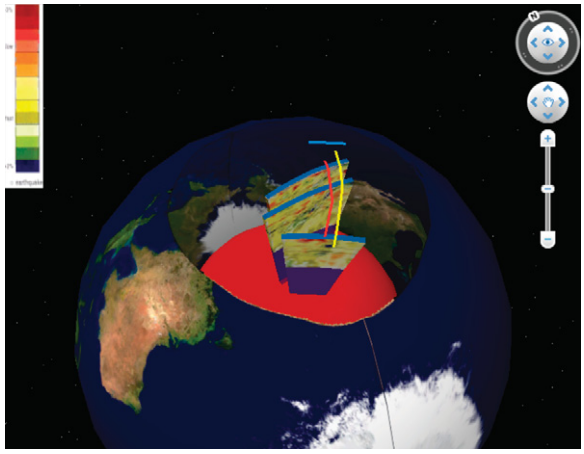

Figure 14. Visualization with circular cutout revealing underlying mantle. Yellow, red, and blue lines mark surface tectonic lineaments. Note that Arctic, North America, and Russia are seen inverted on inner surface of sphere behind core.

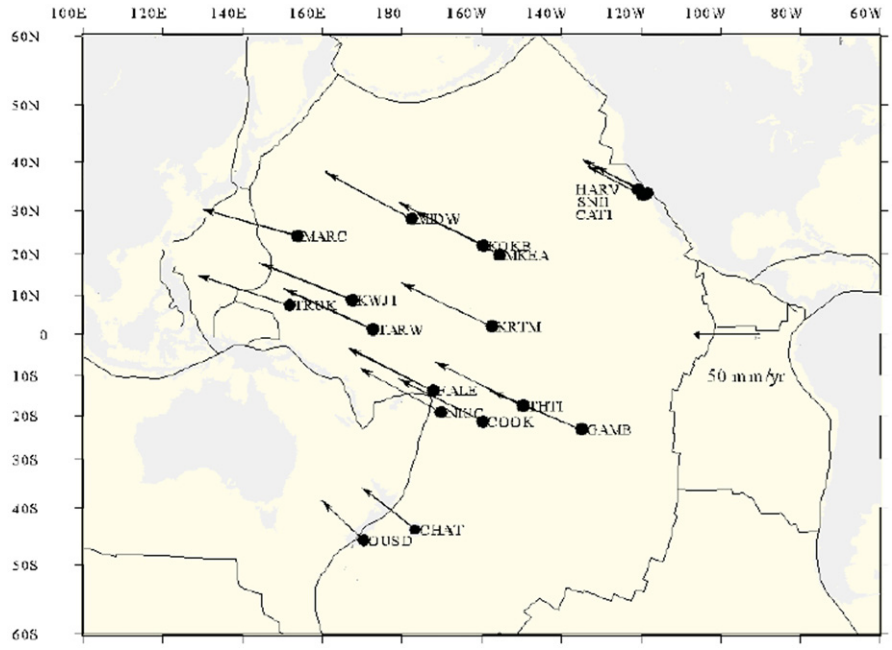

Figure 15. Velocity vectors for the Pacific plate from global positioning system (GPS) station measurements (source: http://cais.gsi.go.jp/Virtual_GSI/Tectonics/Pacific_GPS/index.html).

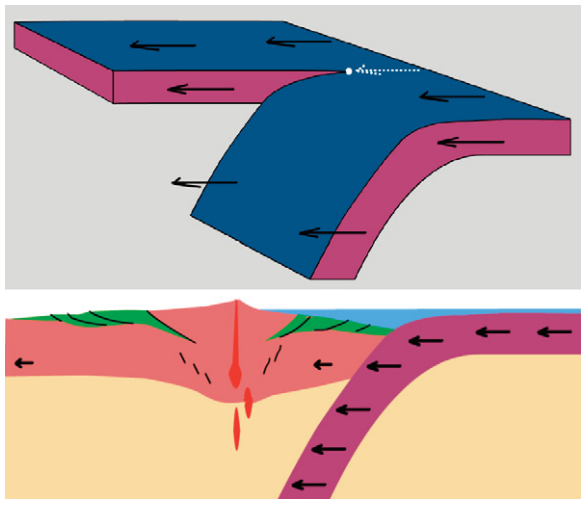

Figure 16. Structure of Andean arc oriented to correspond to polarity of Tonga subduction zone; view is to north. Green denotes forearc and foreland sedimentary basins. Black lines are thrust faults near surface and shear zones at depth. Red denotes magmatism.

zone in model 1 depends on the absolute velocity of the Australian plate west of the study area. Backarc spreading west of Tonga could be compatible with model 1 if the Australian plate drifted west faster than the Pacific plate or if rollback of the opposite-polarity New Hebrides subduction zone west of Fiji created the necessary extension. The direction of absolute plate motion of the Australian plate is northward, approximately perpendicular to the Pacific plate (Kreemer, 2009; Stadler et al., 2010); therefore, it does not have a significant orthogonal component of movement relative to the trench and is equivalent to a stationary block for the purposes of this model. Furthermore, the New Hebrides structure cannot be responsible for all backarc spreading because its influence does not extend beyond the northern end of the Lau Basin. Thus, if model 1 were valid, there ought to be a mountainous magmatic arc bordered by forearc and foreland thrust belts, which are shown in Figure 17, but not seen in ground truth. If there were ever a period during which the tear point drifted passively with the plate or ripped slowly, it could not have lasted long, or a large compressional arc would have grown and endured.

Despite the obvious unlikeliness of model 1 to an expert (professor), we included it among our alternatives in order to challenge novices (students) to think of reasons to reject it, or equivalently, to envisage the types of data that would support it but are not seen.

Model 2. Band-Saw Tearing

Our second model requires an immaterial tear point fixed in an external reference frame (Fig. 18; Supplemental Model 2[2]). The western drift of the Pacific plate can then be compared to pushing a sheet of plywood westward through a band saw and holding the north side level (Fig. 18, inset) while letting the south side sag.

The absolute velocity vector of any material point in the slab in this case would be directed downdip, i.e., parallel to the top and bottom of the slab; consequently, the arc forming above the slab would be under no lateral stress, nei-

[2]Supplemental Model 2. Our second model requires an immaterial tear point fixed in an external reference frame. The absolute velocity vector of any material point in the slab in this case would be directed downdip, i.e., parallel to the top and bottom of the slab. See text for details. See also Figure 18. To download the zip file containing the KML file for Supplemental Model 2, please visit http://dx.doi.org/10.1130/GES00758.S6. Or, to view the html file of Supplemental Models 1–6 with a Google Chrome, Firefox, or Safari web browser, please visit http://dx.doi.org/10.1130/GES00758.S5. Both the html file and the zipped file can also be accessed through the full-text article on www.gsapubs.org.

ther forming an Andean-style compressional structure such as a thrust belt nor an extensional structure such as a backarc spreading ridge. Nevertheless, the model would lead to a prediction of gradual magmatic arc buildup to significant size.

It is not intuitively obvious that there are two independent questions to be addressed in this scenario. First, is the Samoa Archipelago a hotspot trail caused by the Pacific plate drifting slowly westward over a fixed hotspot? And second, has the tear point always been located close to the hotspot? If the latter were true, the tear point southwest of the youngest island, American Samoa, today would have been southwest of the older Western Samoa in the recent past and southwest of the oldest Wallis and Futuna Islands before that, with each of these islands presumed to have formed over the stationary deep mantle hotspot before the younger ones existed. Thus a test of the hotspot trail model would be a progression of island ages and thermally induced decreasing altitudes or bathymetries, comparable to the Hawaiian chain. For a long time, the answer was in doubt because of the occurrence of recent volcanism at both the west and east end of the Samoan volcanic lineament. However, Hart et al. (2004) documented an active submarine volcano east of American Samoa that they named Vailulu'u, and reported isotopic evidence for a Hawaiian-style hotspot trail. Recent volcanism along the Samoan lineament is seen by them as a separate phenomenon superposed on the hotspot progression and therefore requiring a separate explanation.

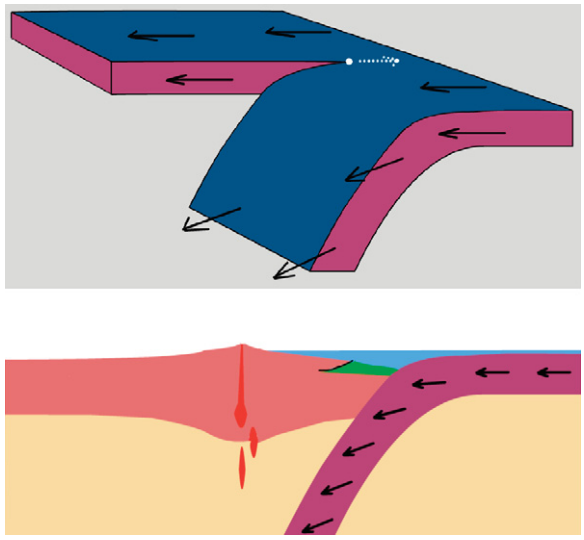

Figure 17. Tear point migrating slowly eastward (white arrow), resulting in dipping absolute movement vectors (black). Green denotes forearc and foreland sedimentary basins. Black line is thrust fault near surface. Red denotes magmatism.

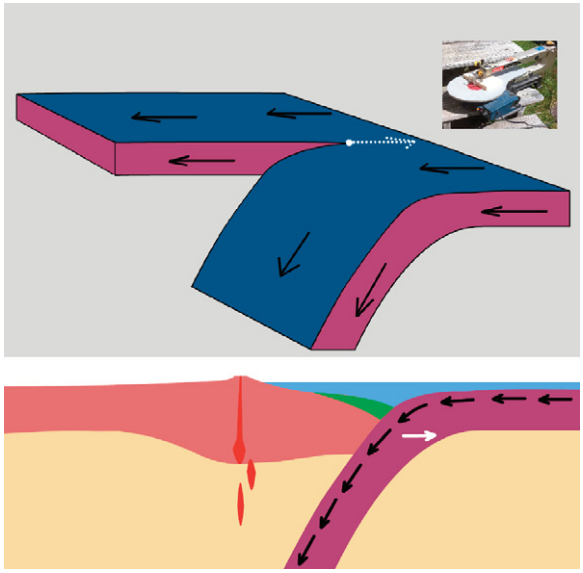

Figure 18. Model 2. Tear point fixed in external reference frame. Velocity (white arrow) is equal and opposite to plate velocity. Velocities in slab are parallel to dip (black arrows). Green denotes forearc and foreland sedimentary basins. Red denotes magmatism. Inset image shows a small carpenter's band saw by analogy.

Model 3. Rapid Rollback

Our third model involves the eastward relative migration of the tear point at a faster rate than the westward absolute movement of the Pacific plate over the hotspot, resulting in eastward absolute movement of the tear point and absolute velocity vectors for material in the slab that are steeper than the slab dip (Fig. 19; Supplemental Model 3[3]). An analogy would be the act of cutting cloth by moving a scissor forward while pulling the cloth backward toward oneself (students have also suggested a comparison with Michael Jackson's moonwalk). In this case, the original tear point would have been at the western end of the Samoan volcanic lineament, well west of the fixed mantle hotspot, and would have migrated rapidly east so that it happens to be close to Vailulu'u today. Rapid migration of the tear point could account for the superposition of recent volcanism on the age progression of the Samoa Archipelago, as discussed here, by flexure of the lithosphere close to the line of tearing. If we could see into the future, the tear point might continue to migrate east of the current hotspot, or its current proximity to the hotspot might trap the tear in a steady-state phase in the future, as represented by model 2.

Since relative motion of the tear point is key, model 3 can also result from modest tear velocities in combination with slow plate velocities. In the end-member case, there is no horizontal component of plate motion and the slab vectors are vertical (Fig. 20). Clearly the Pacific plate has a significant horizontal velocity, so the end-member case is not practical.

Model 4. Deep Mantle Rollback

Model 3 can account for the development of a subduction zone and extensional backarc basin, but we also need to account for the flattening of the slab dip between ~400 and 600 km depth. Kincaid and Olson (1987) suggested that the subduction system may have initially followed model 2 (no rollback), and that rollback and backarc spreading may have ensued when the slab hit the 430–670 km mantle discontinuity after ~10 m.y. at 7 cm/yr. In this scenario,

[3]Supplemental Model 3. Our third model involves the eastward relative migration of the tear point at a faster rate than the westward absolute movement of the Pacific plate over the hotspot, resulting in eastward absolute movement of the tear point and absolute velocity vectors for material in the slab that are steeper than the slab dip. See text for details. See also Figure 19. To download the zip file containing the KML file for Supplemental Model 3, please visit http://dx.doi.org/10.1130/GES00758.S7. Or, to view the html file of Supplemental Models 1–6 with a Google Chrome, Firefox, or Safari web browser, please visit http://dx.doi.org/10.1130/GES00758.S5. Both the html file and the zipped file can also be accessed through the full-text article on www.gsapubs.org.

the slab encounters resistance to subduction due to mid-mantle phase and viscosity changes (430 km is marked by the olivine-spinal transition, whereas the spinel-perovskite transition occurs at 670 km), and it develops a bend that rolls back (lower white arrows in Fig. 21; Supplemental Model 4[4]).

Model 5. Foundering Flat-Slab

As far as we can ascertain, model 5 (Fig. 22; Supplemental Model 5[5]) has not been described in the tectonic literature. In this scenario, the western Pacific plate first cracked along the Tonga Trench and tore at a point to the west of the Samoa Archipelago, causing the southern portion to subduct. A magmatic arc built, but there was no significant backarc spreading. The seamounts and islands of the Samoa Archipelago pierced the plate progressively along a line to the east of the tear point. Islands and seamounts aged and subsided as they drifted westward. At ~6 m.y. ago, the tear point ripped rapidly eastward as in model 3, superimposing recent volcanism of the Vitiaz Lineament and ending in proximity with the hotspot. This rapid rollback resulted in a shallow-dipping slab segment at shallow depth with steep-dipping absolute movement vectors. The flat slab then continued to founder to its present mid-mantle level. In the third dimension, the structure involves a near-pole rotation (cf. De Paor et al., 1989) resulting in the narrowing of Lau Basin toward the south and widening to the north. At ~2 m.y. ago, trench rollback started a near-pole rotation process about an Euler pole located around 24°S; the rotation occurred at a rate of 7°/m.y.

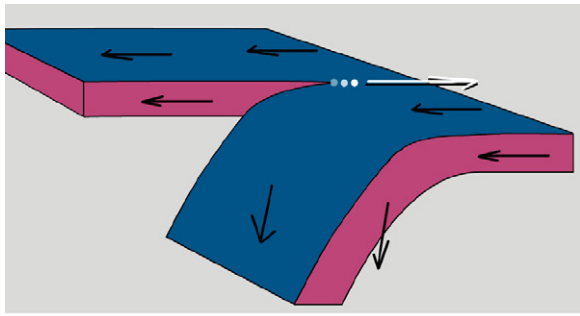

Figure 19. Model 3. Rapid eastward migration of tear point (white arrow). Absolute slab velocity vectors are steeper than slab dip. Stress in arc causes extension and dike intrusions, opening Lau Basin. Red denotes magmatism.

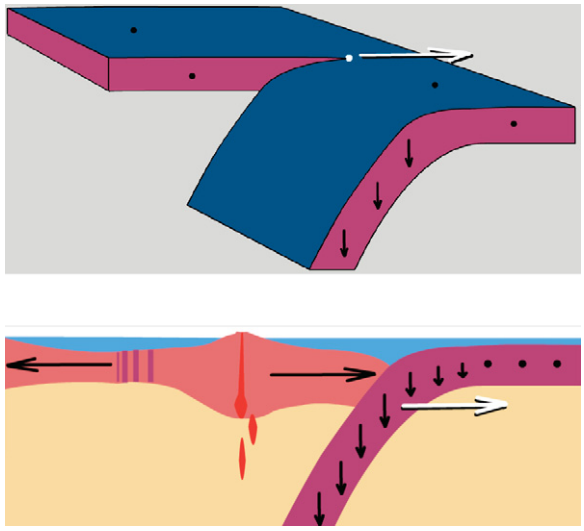

Figure 20. Model 3, continued. Dominance of rollback over horizontal plate motion. Steep to vertical absolute velocities in slab (black arrows). Stress in backarc region is tensional. White arrow denotes velocity of trench rollback; red denotes magmatism.

Model 6. Subduction Step-Back

Our final model is one in which subduction initiates in the west under the Lau arc and then instantaneously steps back to the longitude of the Tonga arc (Fig. 23; Supplemental Model 6[6]). There is no backarc spreading; rather, the marginal basin is floored by a broken-off and abandoned segment of the Pacific plate. This model is established elsewhere: it has been proposed to explain part of the evolution of the Mariana system, among others. However, diffuse magnetic patterns in the Lau Basin imply (Lawver and Hawkins, 1978) that it formed by distributed backarc spreading driven by trench rollback (Uyeda and Kanamori, 1979) and trench suction (Chase, 1978) rather than by entrapment of normal oceanic lithosphere behind a newly formed Tonga arc to its east (these different models of marginal basin formation were discussed in Karig, 1974).

[4]Supplemental Model 4. In this scenario, the slab encounters resistance to subduction due to mid-mantle phase and viscosity changes (430 km is marked by the olivine-spinal transition, whereas the spinel-perovskite transition occurs at 670 km) and it develops a bend that rolls back. See text for details. See also Figure 21. To download the zip file containing the KML file for Supplemental Model 4, please visit http://dx.doi.org/10.1130/GES00758.S8. Or, to view the html file of Supplemental Models 1–6 with a Google Chrome, Firefox, or Safari web browser, please visit http://dx.doi.org/10.1130/GES00758.S5. Both the html file and the zipped file can also be accessed through the full-text article on www.gsapubs.org.

[5]Supplemental Model 5. In this scenario, the western Pacific plate first cracked along the Tonga Trench and tore at a point to the west of the Samoan Archipelago, causing the southern portion to subduct. A magmatic arc built, but there was no significant backarc spreading. At ~6 m.y. ago the tear point ripped rapidly eastward as in model 3. This rapid rollback resulted in a shallow-dipping slab segment at shallow depth with steep-dipping absolute movement vectors. The flat slab then continued to founder to its present mid-mantle level. To download the zip file containing the KML file for Supplemental Model 5, please visit http://dx.doi.org/10.1130/GES00758.S9. Or, to view the html file of Supplemental Models 1–6 with a Google Chrome, Firefox, or Safari web browser, please visit http://dx.doi.org/10.1130/GES00758.S5. Both the html file and the zipped file can also be accessed through the full-text article on www.gsapubs.org.

[6]Supplemental Model 6. Our final model is one in which subduction initiates in the west under the Lau arc and then instantaneously steps back to the longitude of the Tonga arc. There is no backarc spreading; rather, the marginal basin is floored by a broken-off and abandoned segment of the Pacific plate. See text for details. See also Figure 23. To download the zip file containing the KML file for Supplemental Model 6, please visit http://dx.doi.org/10.1130/GES00758.S10. Or, to view the html file of Supplemental Models 1–6 with a Google Chrome, Firefox, or Safari web browser, please visit http://dx.doi.org/10.1130/GES00758.S5. Both the html file and the zipped file can also be accessed through the full-text article on www.gsapubs.org.

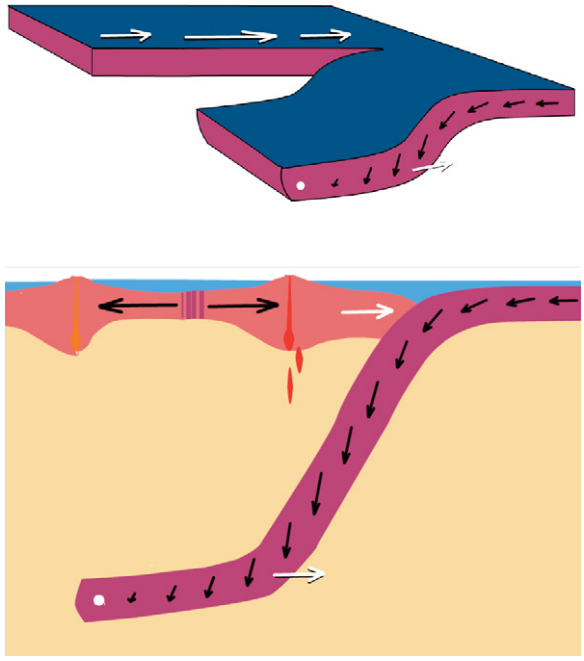

Figure 21. Deep mantle rollback (lower white arrow) may have created flat slab segment at ~600 km and also driving surface rollback (upper white arrow). White spot marks point where slab started to go flat due to mid-mantle resistance. Red denotes magmatism.

We leave the task of debating the fine details of alternate models to regional tectonic experts. As usual, there are end-member cases that can be rejected, but no single hypothesis that trumps all others. Underconstrained alternatives help guide tectonic experts toward the types of data that need to be collected in the future. For instructional purposes, it is useful to present these multiple working hypotheses as examples of the often misunderstood process of science (e.g., Brickhouse, 1990; Handelsman et al., 2004).

DISCUSSION AND CONCLUSIONS

Ever since its inception, Google Earth has been adopted with great enthusiasm by geoscientists (e.g., Butler, 2006), and it has been widely used in geographical and geological education (e.g., Stahley, 2006; Patterson, 2007; Rakshit and Ogneva-Himmelberger, 2008, 2009). Cruz and Zellers (2006) established its efficacy for the study of landforms. COLLADA models have been used in conjunction with Google Earth by many (De Paor et al., 2008, 2009a, 2009b; Selkin et al., 2009; Brooks and De Paor, 2009; Pence et al., 2010; Whitmeyer et al., 2011). Anecdotally, students in several of our classes have reacted positively to the tactile nature of the process of lifting blocks out of the subsurface; they seem to understand the process. However, in order to spur further evaluation studies, there needs to be a greater cohort of academics who create and distribute learning resources for Google Earth using COLLADA and KML.

Previous studies have documented the benefits of learning with visualizations in general (Kali et al., 1997; Orion et al., 1997; Reynolds et al., 2005) and specifically with geographic information systems (Hall-Wallace and McAuliffe, 2002). There are also many studies of the positive role of student research projects in undergraduate education (Libarkin and Kurdziel, 2001; Jenkins et al., 2007). In some cases, instructors already know the right answers, and by mentoring student inquiry rather than just lecturing, they help students to discover those answers. In other cases, questions are more open ended and students discover new findings, thereby acting as genuine researchers as well as learners. This paper presents a case where construction of engaging instructional resources blurred the boundary between academic education and research at the instructor level. It is commonly stated that one does not truly understand any topic until one is asked to teach it. Clearly, the process of preparing course materials is an important aspect of research, and with modern methods of data mining and data visualization, teachers who are not topic experts have the opportunity to help promote not only their own comprehension, but the research community's understanding also.

We are keenly aware of (1) the potential of complex 3D visualizations such as Google Earth to cause visual overload and loss of attention (Rensink et al., 1997; Parkhurst et al., 2002; Martin and Treves, 2008); and (2) the ease with which students can wander off task given simple mouse controls and a whole Earth to explore. Adding emergent blocks to Google Earth helps solve the first problem by creating salience and a focal point for student attention. In separate lab exercises, we use the KML NetworkLink and FlyToView elements as a means of geofencing

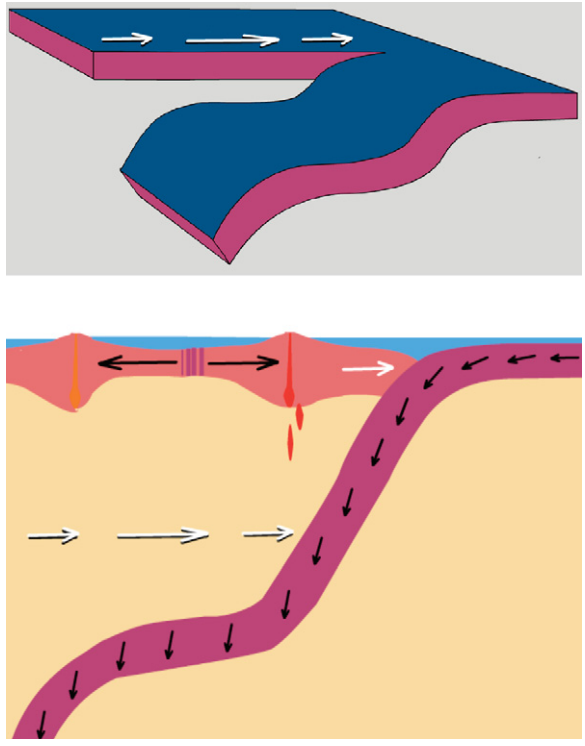

Figure 22. Model 5. Foundered flat slab (see text for discussion). White arrows denote velocity of trench rollback; red denotes magmatism.

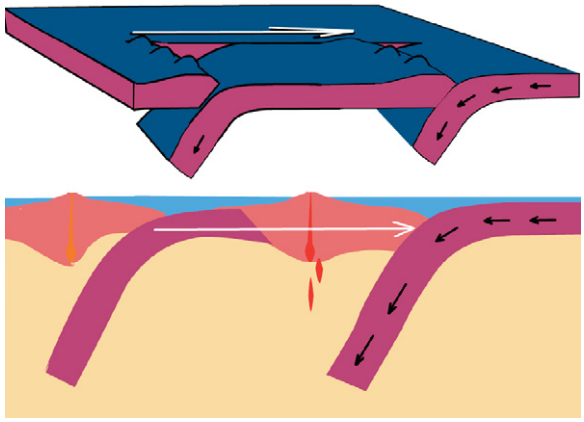

Figure 23. Model 6. Subduction step back. Subduction initiates in west, then steps instantaneously to east (oceanward; see text for discussion). Red denotes magmatism; white arrows denote velocity of trench rollback.

(e.g., Rashid et al., 2006); when a student wanders away from the region the KML script automatically resets the view angle. Serendipitously, our solution to the antimeridian rendering problem in Google Earth reduces visual overload by replacing the complexly overprinted surface imagery and 3D digital elevation model with the simple NASA Blue Marble image of the Earth. Simpson et al. (2012) have taken the concept further by draping a plain beige image over all of the Google Earth surface except for the Archean Kaapvaal craton, which is their area of interest.

Given our recent courses, our classroom use of COLLADA models and Google Earth has been mainly with non-science majors; Goodchild (2006) promoted the notion that general education requires geospatial reasoning as a fourth "R" (in addition to reading, writing, and arithmetic). Furthermore, there is no reason to believe that students majoring in geosciences and other geospatial disciplines would not also benefit. In a previous small (eight student) class of geoscience majors studying structural geology, a student questioned two weeks after the laboratory activity was able to correctly estimate crustal thickness as a proportion of the width of a block. This student might also have been able to give a numerical answer, but evidently had developed a useful visually based mental concept of scale.

We hope that the electronic media links in this paper will lead to widespread dissemination, implementation, and testing of our models in many settings and to the development of new COLLADA models in Google Earth by our colleagues in many second- and third-level educational institutions. Since Google Inc. handed control of KML to the open-source community, its free availability is ensured for the foreseeable future and it has the potential to be truly transformative in the field of geoscience modeling, education, and outreach (De Paor and Whitmeyer, 2011b).

ACKNOWLEDGMENTS

This research was support in part by National Science Foundation (NSF) grants CCLI (Course Curriculum and Laboratory Improvement Program) 0837040, NSF TUES (Transforming Undergraduate Education in Science) 1022755, NSF GEO (Directorate for Geological Sciences) 1034643, and a Google Faculty research award. Any opinions, findings, and conclusions or recommendations expressed in this paper are those of the authors and do not necessarily reflect the views of the National Science Foundation or Google Inc. We thank Old Dominion University students Rajiv Ranasinghe and Whitney Brooke, who participated in initial discussions. We benefitted from long-term collaborations with Steve Whitmeyer, John Bailey, Jennifer Georgen, and Richard Treves, and independent assessor Janice Gobert. We thank the anonymous reviewers for useful suggestions that improved the final manuscript.

REFERENCES CITED

Arnaud, R., and Barnes, M.C., 2006, COLLADA: Sailing the gulf of 3D digital content creation: Wellesley, Massachusetts, A.K. Peters Ltd., 250 p.

Bonnardot, M.-A., Régniera, M., Christovab, C., Ruellana, C.E., and Tric, E., 2009, Seismological evidence for a slab detachment in the Tonga subduction zone: Tectonophysics, v. 464, p. 84–99, doi: 10.1016/j.tecto.2008.10.011.

Brickhouse, N.W., 1990, Teachers' beliefs about the nature of science and their relationship to classroom practice: Journal of Teacher Education, v. 41, no. 3, p. 53–62, doi: 10.1177/002248719004100307.

Brooks, W.D., and De Paor, D.G., 2009, Construction and presentation of Google Earth models for undergraduate education: Geological Society of America Abstracts with Programs, v. 41, no. 7, p. 92.

Butler, D., 2006, Virtual globes: The web-wide world: Nature, v. 439, p. 776–778, doi: 10.1038/439776a.

Chase, C., 1978, Extension behind island arcs and motions relative to hot spots: Journal of Geophysical Research, v. 83, no. B11, p. 5385–5387, doi: 10.1029/JB083iB11p05385.

Cruz, D., and Zellers, S.D., 2006, Effectiveness of Google Earth in the study of geologic landforms: Geological Society of America Abstracts with Programs, v. 38, no. 7, p. 498.

De Paor, D.G., 2007a, The world is (almost) round: An introduction to Google Earth Science: Front Matter Technovations, v. 1, p. 10–11.

De Paor, D.G., 2007b, Embedding Collada models in geobrowser visualizations: A powerful tool for geological research and teaching: Eos (Transactions, American Geophysical Union), v. 88, no. 52, abs. IN32A-08.

De Paor, D.G., 2008a, Enhanced visualization of seismic focal mechanisms and centroid moment tensors using solid models, surface bump-outs, and Google Earth: Journal of the Virtual Explorer, v. 29, paper 2, doi: 10.3809/jvirtex.2008.00195.

De Paor, D.G., 2008b, How would you move Mount Fuji–And why would you want to?: American Geophysical Union, fall meeting, abs. IN44A-05.

De Paor, D.G., and Pinan-Llamas, A., 2006, Application of novel presentation techniques to a structural and metamorphic map of the Pampean Orogenic Belt, northwest Argentina: Geological Society of America Abstracts with Programs, v. 38, no. 7, p. 326.

De Paor, D.G., and Whitmeyer, S.J., 2011a, Geological and geophysical modeling on virtual globes using KML, COLLADA, and Javascript: Computers & Geosciences, v. 37, p. 100–110, doi: 10.1016/j.cageo.2010.05.003.

De Paor, D.G., and Whitmeyer, S.J., 2011b, Transforming undergraduate geoscience education with an innovative Google Earth–based curriculum: American Geophysical Union, fall meeting, no. ED23, abs. 1208428.

De Paor, D.G., and Williams, N.R., 2006, Solid modeling of moment tensor solutions and temporal aftershock sequences for the Kiholo Bay earthquake using Google Earth with a surface bump-out: Eos (Transactions, American Geophysical Union), v. 87, no. 52, abs. S53E–05.

De Paor, D.G., Bradley, D.C., Eisenstadt, G.E., and Phillips, S.M., 1989, The Arctic Eurekan orogen—A most unusual fold and thrust belt: Geological Society of America Bulletin, v. 101, p. 952–967, doi: 10.1130/0016-7606(1989)101<0952:TAEOAM>2.3.CO;2.

De Paor, D.G., Daniels, J., and Tyagi, I., 2007, Five geobrowsing lesson plans: Eos (Transactions, American Geophysical Union), v. 88, no. 52.

De Paor, D.G., Whitmeyer, S.J., and Gobert, J., 2008, Emergent models for teaching geology and geophysics using Google Earth: American Geophysical Union, fall meeting, abs. ED31A-0599.

De Paor, D.G., Brooks, W.D., Dordevic, M.M., Ranashinge, N.R., and Wild, S.C., 2009a, Visualizing the 2009 Samoan and Sumatran earthquakes using Google Earth-based COLLADA models: Eos (Transactions, American Geophysical Union), v. 90, no. 52, abs. U13E-2088.

De Paor, D.G., Whitmeyer, S.J., and Gobert, J., 2009b, Development, deployment, and assessment of dynamic geological and geophysical models using the Google Earth APP and API: Implications for undergraduate education in the Earth and planetary sciences: Eos (Transactions, American Geophysical Union), v. 90, no. 52, abs. ED53E-07.

De Paor, D.G., Dordevic, M., and Wild, S., 2011, Modeling Earth's crust, mantle, and core with Google Mars and Google Moon: Geological Society of America Abstracts with Programs, v. 43, no. 5, p. 243.

Dordevic, M.M., De Paor, D.G., and Whitmeyer, S.J., 2009, Understanding volcanism on terrestrial planets and moons using virtual globes and COLLADA models: Geological Society of America Abstracts with Programs, v. 41, no. 7, p. 260.

Dordevic, M.M., De Paor, D.G., Whitmeyer, S.J., and Beebe, M.R., 2010, Animated COLLADA models and virtual field trips featuring volcanism in various tectonic settings on planet Earth and other rocky planets and moons: Geological Society of America Abstracts with Programs, v. 42, no. 5, p. 420.

German, C.R., Baker, E.T., Connelly, D.P., Lupton, J.E., Resing, J., Prien, R.D., Walker, S.L., Edmonds, H.N., and Langmuir, C.H., 2006, Hydrothermal exploration of the Fonualei Rift and spreading center and the Northeast Lau spreading center: Geochemistry Geophysics Geosystems, v. 7, Q11022, doi: 10.1029/2006GC001324.

Gobert, J., 2000, A typology of models for plate tectonics: Inferential power and barriers to understanding: International Journal of Science Education, v. 22, p. 937–977, doi: 10.1080/095006900416857.

Gobert, J., 2005, Leveraging technology and cognitive theory on visualization to promote students' science learning and literacy, *in* Gilbert, J., ed., Visualization in Science Education: Dordrecht, Springer-Verlag, p. 73–90.

Gobert, J., Wild, S., and Rossi, L., 2012, Testing the effects of prior coursework and gender on geoscience learning with Google Earth, *in* Whitmeyer, S.J., De Paor, D.G., and Bailey, J.E., eds., Google Earth, Virtual Globes, and Virtual Visualizations: Modern Approaches to Geosci-

ence Inquiry and Research: Boulder, Colorado, Geological Society of American Special Paper (in press).

Gudmundsson, O., and Sambridge, M., 1998, A regionalized upper mantle (RUM) seismic model: Journal of Geophysical Research, v. 103, no. B4, p. 7121–7136, doi: 10.1029/97JB02488.

Goodchild, M.F., 2006, The fourth R: Rethinking GIS education: ArcNews, v. 28, no. 3, p. 1.

Goodchild, M.F., 2008, The use cases of digital earth: International Journal of Digital Earth, v. 1, p. 31–42, doi: 10.1080/17538940701782528.

Hall-Wallace, M.K., and McAuliffe, C.M., 2002, Design, implementation, and evaluation of GIS-based learning materials: Journal of Geoscience Education, v. 50, no. 1, p. 5–14.

HandelsIman, J., Ebert-May, D., Beichner, R., Bruns, P., Chang, A., DeHaan, R., Gentile, J., Lauffer, S., Stewart, J., Tilghman, S.M., and Wood, W.B., 2004, Scientific teaching: Science, v. 304, p. 521–522, doi: 10.1126/science.1096022.

Hart, S.R., Coetzee, M., Workman, R.A., Blusztajn, J., Johnson, K.T.M., Sinton, J.M., Steinberger, B., and Hawkins, J.W., 2004, Genesis of the Western Samoa seamount province: Age, geochemical fingerprint and tectonics: Earth and Planetary Science Letters, v. 227, p. 37–56, doi: 10.1016/j.epsl.2004.08.005.

Holt, W.E., 1995, Flow fields within the Tonga slab determined from the moment tensors of deep earthquakes: Geophysical Research Letters, v. 22, p. 989–992, doi: 10.1029/95GL00786.

Isacks, B., Oliver, J., and Sykes, L.R., 1968, Seismology and the new global tectonics: Journal of Geophysical Research, v. 73, p. 5855–5899, doi: 10.1029/JB073i018p05855.

Jenkins, A., Healey, M., and Zetter, R., 2007, Linking teaching and research in disciplines and departments: York, UK, Higher Education Academy, 100 p., http://www.heacademy.ac.uk/research/LinkingTeachingAndResearch_April07.pdf

Kali, Y., Orion, N., and Mazor, E., 1997, Software for assisting high school students in the spatial perception of geological structures: Journal of Geoscience Education, v. 45, p. 10–21.

Karig, D.E., 1974, Evolution of arc systems in the Western Pacific: Annual Review of Earth and Planetary Sciences, v. 2, p. 51–78, doi: 10.1146/annurev.ea.02.050174.000411.

Kincaid, C., and Olson, P., 1987, An experimental study of subduction and slab migration: Journal of Geophysical Research, v. 92, p. 13,832–13,840, doi: 10.1029/JB092iB13p13832.

Kreemer, C., 2009, Absolute plate motions constrained by shear wave splitting orientations with implications for hot spot motions and mantle flow: Journal of Geophysical Research, v. 114, B10405, 18 p., doi: 10.1029/2009JB006416.

Lawver, L.A., and Hawkins, J.W., 1978, Diffuse magnetic anomalies in marginal basins: Their possible tectonic and petrologic significance: Tectonophysics, v. 45, p. 323–339, doi: 10.1016/0040-1951(78)90167-1.

Lay, T., Ammon, C.J., Kanamori, H., Rivera, L., Koper, K.D., and Hutko, A.R., 2010, The 2009 Samoa-Tonga great earthquake triggered doublet: Nature, v. 466, p. 964–968, doi: 10.1038/nature09214.

Libarkin, J.C., and Kurdziel, J.P., 2001, Research methodologies in science education. Assessing students' alternative conceptions: Journal of Geoscience Education, v. 49, no. 4, p. 378–383.

Lupton, J.E., Pyle, D.G., Jenkins, W.J., Greene, R., and Evans, L., 2004, Evidence for an extensive hydrothermal plume in the Tonga-Fiji region of the south Pacific: Geochemistry Geophysics Geosystems, v. 5, Q01003, doi: 10.1029/2003GC000607.

Martin, D.J., and Treves, R., 2008, Visualizing geographic data in Google Earth for education and outreach: American Geophysical Union, fall meeting, abs. IN41B-1145.

McDonald, T.B., and De Paor, D.G., 2008, Above Google Earth: Teaching and research applications of geobrowsers in atmospheric and ionospheric studies: Geological Society of America Abstracts with Programs, v. 40, no. 2, p. 9.

McDougall, I., 2010, Age of volcanism and its migration in the Samoa Islands: Geological Magazine, v. 147, p. 705–717, doi: 10.1017/S0016756810000038.

Moores, E.M., and Twiss, R.J., 1995, Tectonics: New York, W.H. Freeman, 415 p.

Muller, R.D., Sdrolias, M., Gaina, C., and Roest, W.R., 2008, Age, spreading rates and spreading symmetry of the world's ocean crust: Geochemistry Geophysics Geosystems, v. 9, Q04006, doi: 10.1029/2007GC001743.

Mussett, A.E., and Khan, M.A., 2000, Looking into the Earth: An Introduction to Geological Geophysics: Cambridge, UK, Cambridge University Press, 470 p.

Okal, E.A., Fritz, H.M., Synolakis, C.E., Borrero, J.C., Weiss, R., Lynett, P.J., Titov, V.V., Foteinis, S., Jaffe, B.E., Liu, P.L-F., and Chan, I.-C., 2010, Field survey of the Samoa tsunami of 29 September 2009: Seismological Research Letters, v. 81, p. 577–591, doi: 10.1785/gssrl.81.4.577.

Orion, N., Ben-Chiam, D., and Kali, Y., 1997, Relationship between earth-science education and spatial visualization: Journal of Geoscience Education, v. 47, p. 129–132.

Parker, R.L., and Oldenburg, D.W., 1973, Thermal model of ocean ridges: Nature, v. 242, p. 137–139, doi: 10.1038/physci242137a0.

Parkhurst, D., Law, K., and Niebur, E., 2002, Modeling the role of salience in the allocation of overt visual attention: Vision Research, v. 42, p. 107–123, doi: 10.1016/S0042-6989(01)00250-4.

Patterson, T.C., 2007, Google Earth as a (not just) geography education tool: Journal of Geography, v. 106, no. 4, p. 145–152, doi: 10.1080/00221340701678032.

Pelletier, B., and Auzende, J.-M., 1996, Geometry and structure of the Vitiaz Trench Lineament (SW Pacific): Marine Geophysical Researches, v. 18, p. 305–335, doi: 10.1007/BF00286083.

Pence, N., Weisbrot, E., Whitmeyer, S., De Paor, D., and Gobert, J., 2010, Using Google Earth for advanced learning in the geosciences: Geological Society of America Abstracts with Programs, v. 42, no. 1, p. 115.

Rakshit, R., and Ogneva-Himmelberger, Y., 2008, Application of virtual globes in education: Geography Compass, v. 2, p. 1995–2010, doi: 10.1111/j.1749-8198.2008.00165.x.

Rakshit, R., and Ogneva-Himmelberger, Y., 2009, Teaching and Learning guide for application of virtual globes in education: Geography Compass, v. 3, p. 1579–1595, doi: 10.1111/j.1749-8198.2009.00246.x.

Ramos, V.A., and Aleman, A., 2000, Tectonic evolution of the Andes, *in* Cordani, U., et al., eds., Tectonic Evolution of South America: Rio de Janeiro, Brazil, Fundo Setorial de Petróleo e Gás Natural, p. 635–685.

Rashid, O., Mullins, I., Coulton, P., and Edwards, R., 2006, Extending cyberspace: Location based games using cellular phones: Computers in Entertainment, v. 4, article 3C, doi: 10.1145/1111293.1111302.

Rensink, R., O'Regan, J., and Clark, J., 1997, To see or not to see: The need for attention to perceive changes in scenes: Psychological Science, v. 8, p. 368–373, doi: 10.1111/j.1467-9280.1997.tb00427.x.

Reynolds, S.J., Johnson, J.K., Piburn, M.D., Leedy, D.E., Coyan, J.A., and Busch, M.M., 2005, Visualization in undergraduate geology course, *in* Gilbert, J.K., ed., Visualization in Science Education: Netherlands, Springer, Inc., p. 253–266.

Rosenbaum, G., and Lister, G.S., 2004, Neogene and Quaternary rollback evolution of the Tyrrhenian Sea, the Apennines and the Sicilian Maghrebides: Tectonics, v. 23, TC1013, doi: 1010.1029/2003TC001518.

Rosenbaum, G., Gasparon, M., Lucente, F.P., Peccerillo, A., and Miller, M.S., 2008, Kinematics of slab tear faults during subduction segmentation and implications for Italian magmatism: Tectonics, v. 27, TC2008, doi: 10.1029/2007TC002143.

Ryan, W.B.F., Carbotte, S.M., Coplan, J.O., O'Hara, S., Melkonian, A., Arko, R., Weissel, R.A., Ferrini, V., Goodwillie, A., Nitsche, F., Bonczkowski, J., and Zemsky, R., 2009, Global Multi-resolution topography synthesis: Geochemistry Geophysics Geosystems, v. 10, Q03014, doi: 10.1029/2008GC002332.

Selkin, P.A., De Paor, D.G., Gobert, J., Kirk, K.B., Kluge, S., Richard, G.A., and Whitmeyer, S.J., 2009, Emerging digital technologies for geoscience education and outreach: Geological Society of America Abstracts with Programs, v. 41, no. 7, p. 165.

Simpson, C., De Paor, D.G., Beebe, M., and Strand, J., 2012, Transferring maps and data from pre-digital era theses to Google Earth, *in* Whitmeyer, S.J, De Paor, D.G., and Bailey, J.E., eds., Google Earth, Virtual Globes, and Virtual Visualizations: Modern Approaches to Geoscience Inquiry and Research: Boulder, Colorado, Geological Society of America Special Paper (in press).

Smith, G.P., Wiens, D.A., Fischer, K.M., Dorman, L.M., Webb, S.C., and Hildebrand, J.A., 2001, A complex pattern of mantle flow in the Lau backarc: Science, v. 292, p. 713–716, doi: 10.1126/science.1058763.

Stadler, G., Gurnis, M., Burstedde, C., Wilcos, L.C., Alisic, L., and Ghattas, O., 2010, The dynamics of plate tectonics and mantle flow: From local to global scales: Science, v. 329, no. 5995, p. 1033–1038, doi: 10.1126/science.1191223.

Stahley, T., 2006, Earth from above: Science Teacher, v. 73, no. 7, p. 44–48.

Syracuse, E.M., and Abers, G.A., 2006, Global compilation of variations in slab depth beneath arc volcanoes and implications: Geochemistry Geophysics Geosystems, v. 7, p. 1–18, Q05017, doi: 10.1029/2005GC001045.

Uyeda, S., and Kanamori, H., 1979, Back-arc opening and the mode of subduction: Journal of Geophysical Research, v. 84, no. B3, p. 1049–1061, doi: 10.1029/JB084iB03p01049.

van der Hilst, R., 1995, Complex morphology of subducted lithosphere in the mantle beneath the Tonga trench: Nature, v. 374, p. 154–157, doi: 10.1038/374154a0.

Wernecke, J., 2009, The KML handbook: Geographic visualization for the Web: Upper Saddle River, New Jersey, Addison-Wesley, 339 p.

Whitmeyer, S.J., and De Paor, D.G., 2008, Large-scale emergent cross sections of crustal structures in Google Earth: Geological Society of America Abstracts with Programs, v. 40, no. 6, p. 189.

Whitmeyer, S., De Paor, D., Gobert, J., Pence, N., and Liz Weisbrot, E., 2011, Enhancing the geoscience curriculum using geo-browser based learning objects: Proceedings, CCLI/TUES Principal Investigators Conference, Washington, D.C., Abstract no. 638, http://ccliconference.org/abstracts/638.

Yoshii, T., 1975, Regionality of group velocities of Rayleigh waves in the Pacific and thickening of the plate: Earth and Planetary Science Letters, v. 25, p. 305–312, doi: 10.1016/0012-821X(75)90246-0.

Manuscript Received 17 October 2011
Manuscript Accepted 25 November 2011

Geosphere

Emergent and animated COLLADA models of the Tonga Trench and Samoa Archipelago: Implications for geoscience modeling, education, and research

Declan G. De Paor, Steve C. Wild and Mladen M. Dordevic

Geosphere 2012;8;491-506
doi: 10.1130/GES00758.1

Notes